

Adrenal Gland Scintigraphy

Anca M. Avram, MD,* Lorraine M. Fig, MBChB, MPH,*[†] and Milton D. Gross, MD*[†]

There is no question that high-resolution imaging techniques have revolutionized the approach to diagnostic imaging. Computed tomography (CT) and magnetic resonance imaging provide exquisite images of the adrenal glands and offer the best initial imaging approach in the evaluation of patients with suspected adrenal disease. However, an assessment of anatomy is only a portion of the diagnostic effort, which begins with a biochemical evaluation to establish the presence of adrenal gland dysfunction. With a confirmed biochemical diagnosis in hand, a logical and stepwise diagnostic approach can be tailored to a particular patient. Where scintigraphy fits in the evaluation of diseases of the adrenal cortex and medulla in the context of high-resolution imaging and which radiopharmaceuticals should be deployed has changed substantially during the last 2 decades. Adrenal functional imaging has evolved from classic planar scintigraphy to single-photon emission computed tomography (SPECT) and positron emission tomography (PET) using tracers that, by targeting specific metabolic or synthetic processes within the gland, have depicted adrenal pathophysiology. New PET/CT and SPECT/CT technologies integrate anatomic and functional information and redefine the radiotracer principle in the larger context of high resolution anatomic imaging.

Semin Nucl Med 36:212-227 © 2006 Elsevier Inc. All rights reserved.

Adrenal gland scintigraphy uses radiopharmaceuticals with specific imaging characteristics for the adrenal cortex and adrenal medulla. These radiopharmaceuticals enter adrenal hormone synthetic pathways and act as precursor or precursor-like compounds, mimic native hormones, or demonstrate affinity for specific endocrine tissue receptors and, in doing so, provide information regarding target tissue endocrine function(s) (Table 1).^{1,2} Integrating information obtained from anatomic and functional imaging has always been essential for characterization of adrenal disease. Computed tomography (CT) is currently the primary method of imaging the adrenals, and the widespread use of CT technology in clinical practice makes it an ideal instrument for evaluating adrenal gland morphology (Table 2).³ In addition to imaging patients with abnormal adrenal function, the use of CT for general abdominal imaging has led to the incidental discovery of unsuspected adrenal masses (incidentalomas) that, in many patients, require further characterization.

Magnetic resonance imaging (MRI) has value in high-resolution imaging and in tissue characterization and can be used alone or in conjunction with other modalities to evaluate adrenal dysfunction (Table 2).³ Other modalities, such as adrenal vein hormone sampling, have value in selected cases in which neither anatomic nor functional imaging can discern the site(s) of adrenal hormonal hypersecretion. Despite the sharp anatomic detail of CT or MRI, evaluation with adrenal scintigraphy in conjunction with hormonal analysis is used not only in defining the function of adrenal lesions but also in the diagnosis and staging of malignant neoplasms of adrenal origin (Table 3).^{1,4} Positron emission tomography (PET)/CT and single-photon emission computed tomography (SPECT)/CT are new imaging techniques that permit the simultaneous acquisition of anatomic and functional information, resulting in accurate localization and metabolic characterization of pathophysiological processes. The introduction of new radiopharmaceuticals and reintroduction of older radiopharmaceuticals in the context of fused anatomic-functional imaging have considerably expanded the field of adrenal gland scintigraphy. In this review, we discuss adrenal gland imaging and recent developments in the field, with the goal of demonstrating the importance and value of an approach that integrates the functional and anatomic evaluation of adrenal disease.

*Department of Radiology, Division of Nuclear Medicine, University of Michigan, Ann Arbor, MI.

[†]Department of Veterans Affairs Health Systems, Ann Arbor, MI.

Address reprint requests to Anca M. Avram, MD, Division of Nuclear Medicine, Department of Radiology, B1G 505G University Hospital, 1500 E. Medical Center Drive, Ann Arbor, Michigan 48109-0028. E-mail: ancaa@umich.edu

Table 1 Radiopharmaceuticals for Adrenal Gland Imaging

Radiopharmaceutical	Metabolic Activity	Target(s)/Mechanism(s) of Uptake
¹³¹ I-19-iodocholesterol	Uptake mediated by LDL receptor	Adrenal cortex via the LDL-receptor
¹³¹ I-6-iodocholesterol	↓	↓
¹³¹ I-6β-iodomethylnorcholesterol	↓	↓
⁷⁵ Se-selenomethylnorcholesterol	↓	↓
¹³¹ I, ¹²³ I, ¹¹¹ In, ^{99m} Tc-low density lipoproteins	↓	↓
¹²³ I-tyr ³ -octreotide	Somatostatin analog	Neuroendocrine via somatostatin-receptor
¹¹¹ In-/ ¹¹¹ In- DOTA-tyr ³ -octreotide*†	↓	↓
⁹⁰ Y-DOTA-tyr ³ -octreotide*†	↓	↓
⁸⁶ Y-DOTA-tyr ³ -octreotide*†	↓	↓
^{114m} In-octreotide*	↓	↓
⁹⁰ Y-DOTA-lanreotide*†	↓	↓
¹¹¹ In-/ ¹¹¹ In-DOTA-lanreotide†	↓	↓
^{99m} Tc-HYNIC-tyr ³ -octreotide†	↓	↓
¹²³ I-vasoactive intestinal peptide (¹²³ I-VIP)	Hormone	Neuroendocrine via VIP-receptor
¹²³ I-metaiodobenzylguanidine (¹²³ I-MIBG)	Neuronal blocker	Neuroendocrine via active transport into neurosecretory granules
¹³¹ I-metaiodobenzylguanidine (¹³¹ I-MIBG)†	↓	↓
¹²⁵ I-metaiodobenzylguanidine (¹²⁵ I-MIBG)†	↓	↓
¹³¹ I-aminoiodobenzylguanidine (¹³¹ I-AIBG)†	↓	↓
¹¹ C-epinephrine	Catecholamine	↓
¹¹ C-hydroxyephedrine (¹¹ C-HED)	Catecholamine analog	↓
¹¹ C-phenylephrine	Catecholamine analog	↓
¹⁸ F-dopamine	Catecholamine	↓
¹⁸ F-fluorodeoxyglucose (¹⁸ F-FDG)	Glucose analog	Adrenal cortex as a metabolic intermediate
¹¹ C-acetate	TCA intermediate*	↓
¹¹ C-etiomidate	Enzyme inhibitor	Adrenal cortical enzyme inhibitor
¹¹ C-metiomate	↓	↓
¹³¹ I-metyrapone	↓	↓

Reprinted with permission from Gross et al.⁴

LDL, low-density lipoprotein.

*Therapeutic or potential therapeutic radiopharmaceutical.

†Tricarboxylic acid cycle intermediate.

Physiological Basis of Functional Adrenal Imaging

The adrenal glands are paired retroperitoneal endocrine structures localized superior and medial to the kidneys. The adrenal glands consist of 2 embryologically, morphologically, and functionally distinct units: the adrenal cortex, which is of mesodermal origin and secretes steroid-derived hormones, and the medulla, which is of neural crest origin and secretes norepinephrine and epinephrine. The adrenal cortex contains 2 regions: the subcapsular zona glomerulosa, which secretes mineralocorticoids (principally aldosterone) and the deeper zona fascicularis and reticularis, which secretes glucocorticosteroids (principally cortisol) and weak androgens (dehydroepiandrosterone [DHEA], dehydroepiandrosterone sulfate [DHEA-S], and androstenedione).

Steroid hormone biosynthesis starts with cholesterol delivered to the adrenal cortical cells by circulating low-density lipoproteins. Cholesterol analog, like ¹³¹I-6β-iodomethyl-19-norcholesterol (NP-59), are incorporated in low-density lipoproteins and accumulated by adrenocortical cells

through a receptor-mediated process.⁵ Once located within the adrenal cortex, the 19-norcholesterol derivatives are esterified, like native cholesterol, but are not further metabolized. In the syndromes of excess production of glucocorticoids, mineralocorticoids, and adrenal androgens, NP-59 uptake is facilitated by adrenocorticotrophic hormone (ACTH) in the inner zones of the cortex and the rennin-angiotensin system in the outer cortex and has been shown to be quantitatively related to steroid hormone output.^{5,6} Drugs and conditions that interfere with adrenocortical uptake of NP-59 are listed in Table 4.

The adrenal medulla synthesizes catecholamines (norepinephrine and epinephrine) that are stored in membrane-bound storage vesicles in association with soluble proteins (chromogranins) and nucleotides forming the neurosecretory granules. Under neural or humoral (eg, angiotensin, serotonin, histamine) stimulation, catecholamines are released from the vesicles by exocytosis and diffuse into the circulation. Within the medulla, catecholamines are recycled and restored in secretory vesicles by an energy-dependent type I uptake mechanism specific to the adrenal medulla and sym-

Table 2 Adrenal Gland Anatomic Imaging Techniques

Technique	Principle	Advantages	Disadvantages	Comments
Ultrasound	Reflection of ultrasound, depicts anatomy	Widely available, no radiation exposure	Limited resolution. Interference by fat and bowel gas	Limited utility
Angiography	X-ray attenuation with iodinated contrast, depicts vascular anatomy	Detailed depiction of vascular anatomy	Invasive (arterial puncture). Technically demanding. May cause adrenal hemorrhage or infarction. Risks of contrast reaction	Generally obsolete for adrenal localization
CT	X-ray attenuation, anatomy based (iodinated contrast may be used)	Highest spatial resolution. X-ray attenuation and washout of contrast can be quantified	May fail in postoperative or very thin patients. Radiation exposure.	Very widely used
MRI	Radiofrequency signal by protons in magnetic field following radiofrequency stimulus	High spatial resolution. No ionizing radiation. Some degree of tissue characterization	Limited specificity of tissue characterization. Resolution < CT in routine adrenal imaging applications.	Limited advantages over CT. Modes of tissue characterization may be useful.

pathetic nervous system. Circulating catecholamines are inactivated by a type II uptake mechanism in the extra-adrenal and extraneuronal tissues, followed by rapid metabolic conversion to metanephrines.

Metaiodobenzylguanidine (MIBG) is a guanethidine analog that structurally is similar to norepinephrine. It is recognized by type I uptake mechanism and stored in the catecholamine storage vesicles and has been used to image the adrenal medulla and sympathomimetic tissues for more than 20 years.⁷⁻⁹ There are certain medications that interfere with MIBG uptake and should be avoided before MIBG imaging (Table 5). With the exception of labetalol, which has an inhibitory action on the type I uptake mechanism, adrenergic blockade does not interfere with the uptake of MIBG, and clinical studies can be safely performed during treatment for hypercatecholaminemia.¹⁰⁻¹² New positron-emitting radionuclides that target the catecholamine synthesis or reuptake pathway include ¹¹C-epinephrine, ¹¹C-hydroxyepinephrine, ¹⁸F-fluorodopamine (¹⁸F-FDA), and ¹⁸F-fluorodihydroxyphenylalanine (¹⁸F-DOPA). These tracers are catecholamines or catecholamine analogs that are actively transported in the neurosecretory granules via the type I uptake mechanism and, by exploiting the high spatial resolution of PET technology, have demonstrated high sensitivity and specificity for localization of pheochromocytomas.¹³ Among these agents, ¹⁸F-FDA has been shown to be superior to ¹³¹I-MIBG for localization of metastatic pheochromocytoma.¹⁴ However, some malignant pheochromocytomas have failed to concentrate both MIBG and ¹⁸F-FDA and have been imaged with ¹⁸F-fluorodeoxyglucose (FDG) or ¹¹¹In-pentetreotide, which likely are related to tumor dedifferentiation and lack of catecholamine uptake mechanism expression.^{15,16}

FDG is a nonspecific tumor imaging agent that has become the primary positron-emitting radionuclide and is used widely in the diagnosis and staging of a variety of malignancies. FDG is a glucose analog, enters the cells like glucose, is

Table 3 Clinical Utility of Adrenal Scintigraphy

Adrenal Cortex
Distinguishing unilateral from bilateral adrenocortical disease
Autonomous asymmetric, bilateral adrenal hyperplasia in hypercortisolism (NP-59, SMC)
Subtle bilateral adrenal hyperplasia in primary aldosteronism (NP-59, SMC)
Identifying the adrenal contribution to hyperandrogenism (NP-59)
Depicting adrenal cortical function
Identifying function in benign vs space occupying/malignant or metastatic unilateral and bilateral incidentally discovered adrenal masses (NP-59, SMC, FDG)
Identifying function in adrenocortical re-implants after bilateral adrenalectomy (NP-59, SMC)
Identifying adrenocortical function after intra-arterial alcohol infusion for ablation (NP-59, SMC)
Preoperative identification of suppression of normal contralateral adrenal function (NP-59, SMC)
Predict incidentally discovered masses with potential to progress to autonomous adrenal function
Adrenal Medulla/Neuroendocrine
Depicting sources of hypercatecholaminemia
Intra-adrenal/extra-adrenal/metastatic/familial pheochromocytomas (MIBG, OCT, FDG, EPI, HED)
Other neuroendocrine neoplasms
Neuroblastoma, non-hypersecretory pheochromocytoma/paragangliomas (MIBG, OCT, FDG, EPI, HED)
Medullary thyroid carcinoma, carcinoid, etc (OCT)

Reprinted with permission Gross et al.⁴

NP-59, ¹³¹I-6 β -iodomethyl-norcholesterol; [†]SMC, ⁷⁵Se-selenomethyl-norcholesterol; FDG, ¹⁸F-fluorodeoxyglucose; MIBG, ¹³¹I(¹²³I)-meta-iodobenzylguanidine; OCT, ¹²³I, ¹¹¹In-octreotide and analogs; EPI, ¹¹C-epinephrine; HED, ¹¹C-hydroxyephedrine.

Table 4 Drugs That Interfere With NP-59 Uptake*

Drug	Mechanism
Spironolactone	Aldosterone receptor blocker, stimulation of aldosterone secretion
Ketoconazole	Suppression of cortisol biosynthesis/secretion
Diuretics; oral contraceptives	Stimulate renin/angiotensin secretion
Glucocorticoids (eg, dexamethasone)†	Suppression of ACTH/cortisol biosynthesis
Cholesterol-lowering agents	Decrease cholesterol/stimulate LDL receptor
Hypercholesterolemia/genetic	Decrease LDL receptor activity

LDL, low-density lipoprotein.

*These medications should be discontinued for 4 to 6 weeks before imaging.

†Studies may be intentionally performed with dexamethasone suppression.

phosphorylated by hexokinase to FDG-6-phosphate, and is trapped within the cancer cell. Because of the relative lack of glucose-6-phosphatase in the cancer cells as compared with normal tissues, there is focal intracellular FDG accumulation, resulting in high tumor/background uptake ratios. FDG has demonstrated great clinical utility in detection of adrenal gland malignancies, both primary and metastatic tumors, with a reported sensitivity of 100%, specificity 94%, and accuracy 96%.¹⁷ The clinical procedures and the radiopharmaceuticals currently used in adrenal gland scintigraphy are described in Table 6.

Functional Imaging of Cushing Syndrome

Cushing syndrome is characterized by excess cortisol production, which often is associated with varying degrees of adrenal androgen overproduction. Cushing syndrome may result from stimulation of adrenal glands by excess ACTH from the pituitary (ACTH-producing pituitary adenoma) or from an extrapituitary tumor (ectopic ACTH syndrome, eg, small cell lung cancer, carcinoid, medullary thyroid cancer, other neuroendocrine tumors). In such instances, the syndrome is called ACTH-dependent Cushing syndrome. Excess ACTH secretion leads to functional hypertrophy of the adrenal glands. The scintigraphic pattern characteristic for ACTH-dependent Cushing syndrome is symmetric to varying degrees of asymmetric, bilateral visualization of the adrenal glands on NP-59 imaging (Fig. 1).

The availability of sensitive ACTH assays and the routine use of anatomic imaging techniques for detection of pituitary adenomas and other ACTH-secreting tumors have reduced

the use of adrenal scintigraphy for the diagnosis of ACTH-dependent Cushing syndrome.

Anatomic imaging in ACTH-dependent Cushing syndrome may show normal adrenals (in 30% of cases) or diffuse bilateral enlargement (in 70% of cases) and the mean width of the adrenal limbs correlated with the circulating cortisol and ACTH levels.¹⁸ In the evaluation of patients with persistent cortisol excess after bilateral adrenalectomy for ACTH-dependent Cushing syndrome, NP-59 scintigraphy has been used for identification of adrenal remnants and to guide surgical intervention (Fig. 2).

ACTH-independent Cushing syndrome can result from an adrenal adenoma, adrenal carcinoma, or bilateral nodular adrenal hyperplasia. The scintigraphic pattern of adrenal adenoma is unilateral visualization of the gland containing the adenoma; the contralateral gland is not visualized because it is hypofunctional and atrophic as the result of prolonged ACTH suppression by autonomous cortisol secretion from the adrenal adenoma (Fig. 3). In adrenal carcinoma, there is nonvisualization of the adrenal glands bilaterally. These tumors do accumulate radiocholesterol but usually have insufficient tracer uptake for visualization on scintigraphy. However, tumoral glucocorticoid secretion is sufficient to cause hypercortisolism, suppress pituitary ACTH production, and radiocholesterol accumulation by the contralateral adrenal gland.¹⁹ The degree of cellular differentiation may play a role in whether an adrenal carcinoma will accumulate sufficient radiocholesterol for imaging, and rare, well-differentiated tumors have imaged with NP-59.²⁰

Bilateral nodular adrenal hyperplasia is characterized by

Table 5 Drugs that interfere with MIBG Uptake*

Drug	Mechanism
Tricyclic antidepressants, cocaine, labetalol	Inhibition of type I amine uptake mechanism
Norepinephrine, serotonin, guanethidine	Neurosecretory granule uptake competition
Reserpine, labetalol, symapthomimetic amines (eg, phenylephrine, ephedrine, pseudoephedrine, phenylpropanolamine, cocaine)	Neurosecretory granule content depletion
Calcium-channel blockers (eg, diltiazem, nifedipine, verapamil)	Uncertain mechanism (also enhance retention of previously stored NE and MIBG by blocking Ca ²⁺ -mediated release from granules)

NE = norepinephrine.

*These medications should be discontinued for 1 week, with the exception of labetalol and reserpine, which should be discontinued for 4 weeks before imaging.

Table 6 Techniques of Adrenal Scintigraphy

	NP-59	¹³¹ I-MIBG	¹²³ I-MIBG†	¹¹¹ In-pentetreotide	¹⁸ F-FDG
Thyroid blockade* (SSK1 1 drop or Lugol's 2 drops in beverage tid)	Start 2 days before injection and continue for 14 days	Start 2 days before injection and continue for 6 days	Start 2 days before injection and continue for 4 days	Not required	Not required†
Adult dose (iv)	37 MBq	18.5 MBq-37 MBq	370 MBq	222 MBq	555 MBq
Shelf-life	2 weeks; frozen	2 weeks; 4 C	24 h; 4 C	6 h; room temp	110 min; room temp
% Uptake/adrenal	0.07-0.26%	0.01-0.22%	0.01-0.22%	–	–
Dosimetry (cGy/dose)	–	From package insert	From package insert	–	–
Adrenal	28-88	0.38-0.75	8-28	1.51	0.12
Ovaries	8.0	0.14-0.27	0.35	0.98	0.11
Liver	2.4	1.45-2.90	0.32	2.43	0.24
Kidneys	2.2	0.16-0.32	–	10.83	0.21
Spleen	2.7	1.10-2.20	–	14.77	0.15
Urinary bladder	–	1.40-2.80	–	6.05	0.73
Thyroid	150	0.17-0.33	17.7	1.49	0.12
Whole body	1.2	–	0.29	–	0.12
Effective dose equivalent	–	0.35-0.70	–	2.61	0.19
Beta emission	Yes	Yes	No	No	No
Laxatives (eg, bisacodyl 5-10 mg p.o. bid)	Begin 2 days before and continue during imaging	Begin postinjection	Begin postinjection	Begin postinjection	No 2 days preinjection
Imaging interval post-radiotracer administration (optional additional imaging times)	Non-DS; one or more days 5, 6, or 7 postinjection DS: one or more early: (3), 4 and one or more late; 5, 6, or 7 days postinjection	24, 48 (72) hours postinjection	2-4, 24 (48) hours postinjection	4-6, 24, (48) hours postinjection	60 min postinjection None
Collimator	High-energy, parallel-hole	High energy, parallel-hole	Low-energy, parallel-hole	Medium-energy, parallel-hole	None
Principal photopeak (abundance)	364 keV (81%)	364 keV	159 keV	172 keV (90%), 245 keV (94%)	511 keV positron tomography
Window	20% window	20% window	20% window	20% window	
Imaging time/counts (per view)	20 min/100 K	20 min/100 K	10 min (at 3 h): 20 min/1M (±SPECT)	Head and neck: 10-15 min/300 K (at 4-24 h) and 15 min/200 K (at 48 h) Chest and abdomen: 10 min/500 K (±SPECT)	5 min/bed position × 4 positions 3D images

DS, dexamethasone suppression; K, thousand counts; M, million counts.

Modified with permission from Kloos RT, Khafagi F, Gross MD, et al: Adrenal (Section 10), in Maisey MN, Britton KE, Collier DB (eds): Clinical Nuclear Medicine (ed 3). London, Chapman and Hall, 1998, p 359

*Patients allergic to iodine may be given potassium perchlorate 200 mg every 8 hours after meals or triiodothyronine 20 mg every 8 hours.

†0-1.4%¹²⁵I contamination.

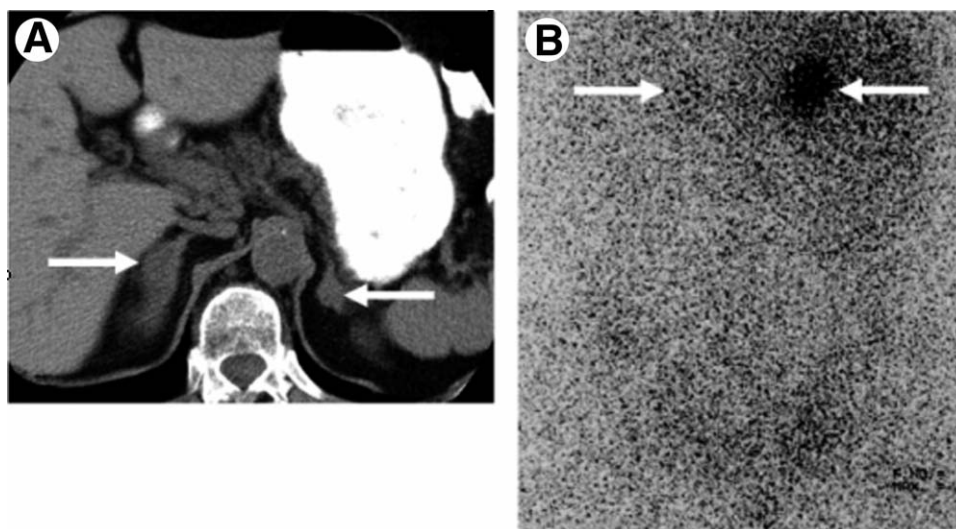


Figure 1 Bilateral, asymmetric ACTH-dependent nodular hyperplasia causing Cushing's syndrome in a 73-year-old woman. (A) CT demonstrates bilateral nodular enlargement of the adrenals, 4.6 cm on the right and 1.3 cm on the left (arrows). (B) Posterior NP-59 scan demonstrates marked asymmetry with faint but discernible accumulation in the smaller left adrenal as compared with the right adrenal (arrows). (Reprinted with permission from Rubello et al.⁸ © 2002 Society of the European Journal of Endocrinology.)

bilateral asymmetric visualization of the adrenal glands (Fig. 4). Functional imaging is most important in these cases because anatomic imaging may cause the misidentification of only the largest adrenal nodule as a unilateral adenoma, failing to correctly denote the bilateral nature of the process in as many as 40% of cases.²⁰ Correlation of anatomic and functional information will avoid an inappropriate and noncurative, unilateral adrenalectomy. Table 7 summarizes the imaging patterns in Cushing syndrome.

Functional Imaging of Primary Aldosteronism

Primary aldosteronism is defined as excess aldosterone secretion resulting in hypertension and hypokalemia. The adrenal pathology underlying this syndrome is either an aldosterone-secreting cortical adenoma (usually <2 cm in diameter) or bilateral hyperplasia of the zona glomerulosa. Biochemical diagnosis demonstrating increased levels of plasma and/or urinary aldosterone

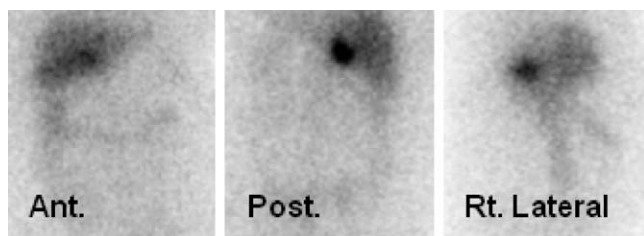


Figure 2 Anterior (Ant), posterior (Post), and right lateral (Rt. Lateral) abdominal NP-59 images demonstrate intense, focal uptake in the right adrenal fossa in a 23-year-old woman with an incompletely resected pituitary neoplasm and hypercortisolism 12 months after bilateral adrenalectomy. This is an example of recurrent hypercortisolism caused by ACTH stimulation of an adrenal remnant. Abdominal CT did not identify adrenal tissue in either adrenal fossae.

levels and suppressed plasma renin activity should always precede imaging.

Scintigraphy in hyperaldosteronism is facilitated with the use of dexamethasone administration (1 mg orally every 6 hours for 7 days before NP-59 injection and throughout the imaging period) with the goal of suppressing the ACTH-dependent component of radiocholesterol uptake occurring in the zona fasciculata. This dexamethasone regimen delays visualization of normal adrenals until at least 5 days after radiocholesterol injection. Visualization of adrenals at or beyond 5 days is called "breakthrough" and reflects the 50% uptake of radiocholesterol that is ACTH independent in normal adrenal tissues. Early visualization

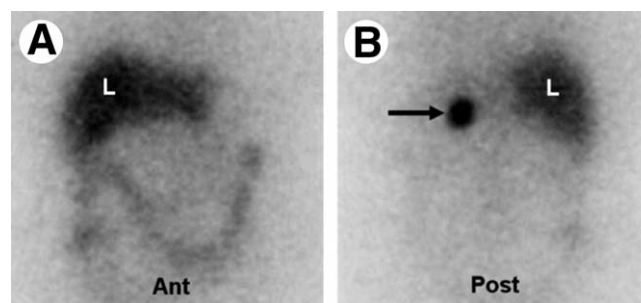


Figure 3 Adrenocortical adenoma causing Cushing's syndrome, depicted by NP-59. Shown are the (A) Anterior (Ant) and (B) posterior (Post) abdominal NP-59 scans of a 48-year-old woman with ACTH-independent Cushing's syndrome and a 3-cm left adrenal mass on CT scan that proved to be an adrenocortical adenoma. The black arrow indicates left-sided, intense adrenal uptake. Note the absence of right adrenal NP-59 uptake as a result of ACTH suppression. There is normal uptake in liver (L) and colon in the anterior projection. (Reprinted with permission from Rubello et al.⁸ © 2002 Society of the European Journal of Endocrinology.)

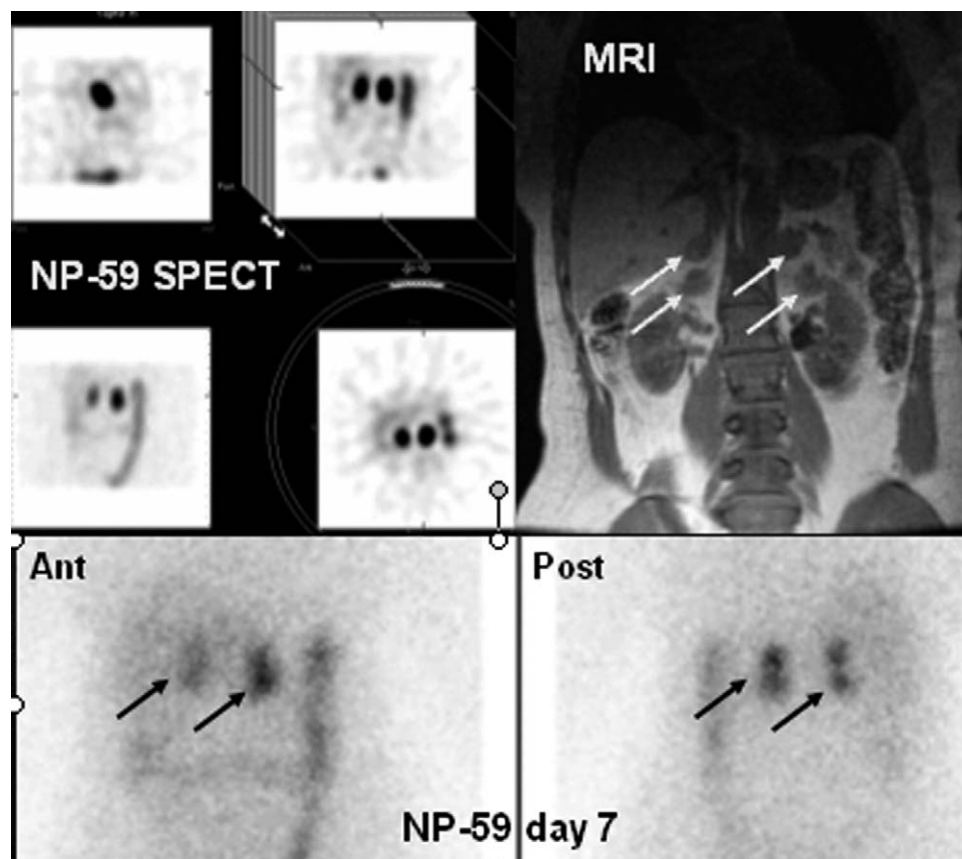


Figure 4 NP-59 scan (SPECT and planar images) demonstrating bilateral macronodular adrenal hyperplasia in a 60-year-old woman presenting with bilateral nodular enlargement of the adrenals on cross-sectional anatomic imaging and biochemical evidence of ACTH-independent Cushing syndrome. MRI demonstrates 2 nodular masses involving each adrenal gland.

(before the fifth day after injection) in a unilateral pattern (aldosteronoma; Fig. 5) or bilateral pattern (adrenal hyperplasia; Fig. 6) before day 5 after injection is the hallmark of primary aldosteronism. For high diagnostic accuracy, medications that may increase radiocholesterol uptake in normal adrenal tissues, such as spironolactone, diuretics, and oral contraceptives (Table 3), should be discontinued 4 to 6 weeks before imaging. Table 8 summarizes the imaging patterns in primary aldosteronism.

Functional Imaging of Hyperandrogenism (Virilization)

Excessive androgen production can be the result of excess secretion from the ovaries, adrenals, or peripheral conversion of precursor steroids to androgens. Patients in whom an adrenal source of androgen hypersecretion is suspected can be evaluated with NP-59 scintigraphy. Dexamethasone suppression should be used to accentuate activity observed in

Table 7 Scintigraphy in Cushing's Syndrome

Scintigraphic Pattern	Type of Cushing Syndrome
Bilateral symmetrical imaging	ACTH-dependent Cushing: hypothalamic; pituitary Cushing's disease; ectopic ACTH syndrome; ectopic CRF syndrome
Bilateral asymmetrical imaging	ACTH-independent Cushing: Bilateral nodular hyperplasia*
Unilateral imaging	Adrenal adenoma†; adrenal remnants‡; ectopic adrenocortical tissue‡
Bilateral nonvisualization	Adrenal carcinoma*¶; severe hypercholesterolemia§

CRF, corticotropin-releasing factor.

*Almost always asymmetrical.

†Cortisol secreting lesions suppress tracer uptake into contralateral gland.

‡Usually only one focus present, occasionally more than one focus may be present in ectopic locations or metastatic sites.

§A potential cause for interference with the effectiveness of study.

¶Very rarely tumors (and metastases) may accumulate sufficient tracer to image.

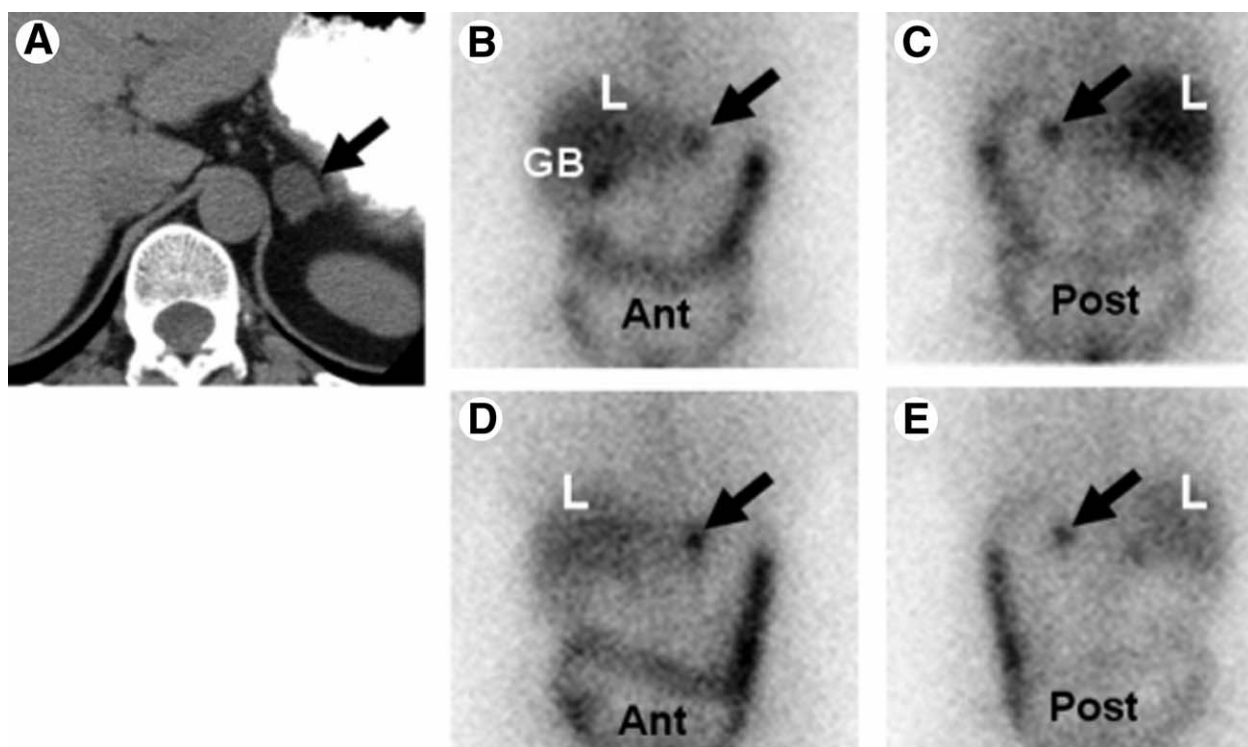


Figure 5 Left adrenal aldosteronoma depicted with dexamethasone suppression NP-59 imaging. A 57-year-old woman with biochemical evidence of hyperaldosteronism and a left adrenal mass. Abdominal CT (A) demonstrates a 2-cm left adrenal mass (black arrow). Shown are the anterior (B, Ant) and posterior (C, Post) abdominal NP-59 scans on the third day after injection and anterior (D) and posterior (E) abdominal NP-59 scans on the fifth day after injection. Abnormal left adrenal uptake (black arrows) occurs early, before day 5 after injection (B and C). Normal uptake in liver (L), bowel (B), and gallbladder (GB). (Reprinted with permission from Rubello et al.⁸ © 2002 Society of the European Journal of Endocrinology.)

autonomous adrenal tissues while suppressing physiologic activity in the ACTH-dependent zona fascicularis.

Three patterns of adrenocortical visualization (on dexamethasone suppression) were demonstrated in a study of 37 women with varying degrees of hyperandrogenism: Early bilateral visualization (<5 days) was found in 15 patients, and adrenal vein testosterone gradients were found in 6 of 6 patients where these measurements were made, confirming bilateral zona reticularis adrenal hyperplasia. In 5 patients, early (<5 days) unilateral or markedly asymmetric adrenal visualization was seen, and adrenal adenomas were confirmed in 4 of the 5 patients. In the remaining 17 patients, bilateral late visualization was observed (>5 days), and these scans were considered normal.²¹ Occasionally, NP-59 imaging has been successfully used in the identification of both ovarian (arrhenoblastoma) and testicular neoplasms.²²⁻²⁴

A new approach to functional imaging of the adrenal cortex used PET with ¹¹C-metomidate (MTO).²⁵⁻²⁷ MTO binds specifically to ¹¹β-hydroxylase (CYP 11B1, P450_{11β}), an enzyme that is essential in the biosynthesis of cortisol and aldosterone and regulated by ACTH. Because of its highly specific targeting, MTO has been used to distinguish lesions of adrenocortical origin. In a study of 16 patients with adrenal masses ¹¹C-MTO clearly separated 13 adrenocortical lesions (including both nonsecreting and hypersecretory lesions represented by cortical adenomas, cortical carcinoma, and macronodular hyperplasia) from 3 noncortical lesions (benign

and malignant pheochromocytoma and metastasis to the adrenal). However, ¹¹C-MTO PET could not distinguish benign adrenocortical tumors and adrenocortical cancer.²⁶ In this study, FDG-PET separated all malignant lesions from benign adrenal masses, showing a specificity, sensitivity, and diagnostic accuracy of 100% for characterization (malignant versus benign) of adrenal masses.²⁶

Another study comparing the results of ¹¹C-MTO PET and FDG-PET for evaluation of adrenal lesions studied 21 patients with incidentally discovered adrenal masses, including both hormonally active and inactive adrenal adenomas, adrenal cancer, pheochromocytoma, cyst, lipoma, lymphoma, and adrenal metastases.²⁷ ¹¹C-MTO identified all lesions of adrenocortical origin, with the highest tracer uptake (expressed as standardized uptake value [SUV]) in adrenocortical carcinoma (SUV_{median} 28), followed by hypersecretory cortical adenomas (SUV_{median} 12.7) and nonsecretory adenomas (SUV_{median} 12.2); the noncortical tumors demonstrated SUV_{median} 5.7. ¹⁸F-FDG-PET showed increased tracer activity in pheochromocytomas and adrenocortical carcinoma, but all inactive adenomas and most hypersecreting adenomas were difficult to detect against background activity.²⁷

The Incidentally Discovered Adrenal Mass (Adrenal Incidentaloma)

Adrenal adenomas are relatively common (2-9%) in the general population, and the routine use of high-resolution imag-

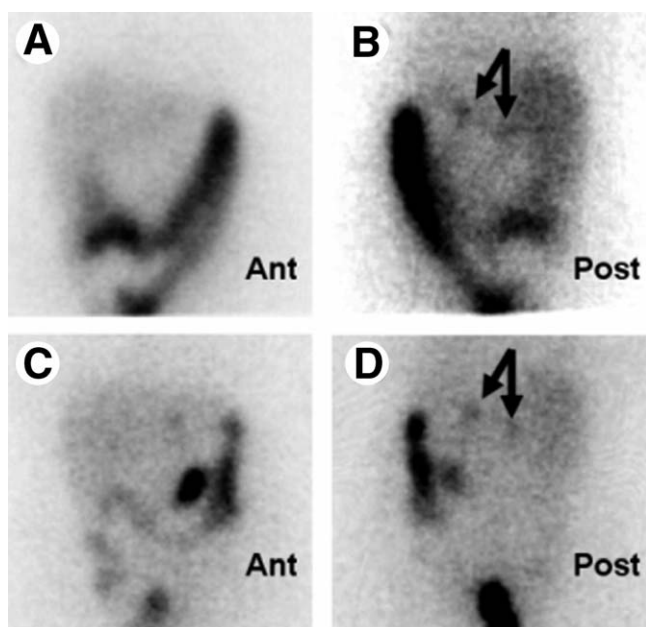


Figure 6 Bilateral adrenal hyperplasia causing primary hyperaldosteronism in a 35-year-old woman with hypertension, biochemical evidence of hyperaldosteronism, and an outside CT report of bilateral adrenal thickening. Shown are the anterior (A, Ant) and posterior (B, Post) abdominal NP-59 scan on the fourth day after injection and the anterior (C) and posterior (D) abdominal NP-59 scans on the fifth day after injection. Bilateral adrenal visualization on day 4 confirmed on day 5 after injection (black arrows) documents bilateral hyperfunction. (Reprinted with permission from Rubello et al.⁸ © 2002 Society of the European Journal of Endocrinology.)

ing techniques (ultrasound, CT, and MRI) for evaluation of abdominal symptoms leads to identification of many unsuspected adrenal lesions.¹⁷ These lesions require further investigation for detecting hormonal hypersecretion and for making the critical distinction between benign and malignant lesions. In the absence of a known malignancy, 70% to 94% of adrenal incidentalomas are nonsecreting benign adenomas.²⁸ In the clinical setting of a known extra-adrenal malignancy, 50% are adrenal metastases, mostly derived from carcinomas of the lung, breast, stomach, ovary, and kidneys, as well as leukemia, lymphomas, and melanomas. Other adrenal masses seen in decreasing prevalence are adrenal cysts in 4% to 22%, myelolipoma in 7% to 15%, and pheochromocytoma in 0% to 11%.²⁸

Diagnostic evaluation of adrenal incidentalomas begins with biochemical evaluation to assess for hormone hypersecretion because hormonally active adrenal masses require

surgical excision. Laboratory screening should consider a functional analysis of all zones of the adrenal cortex and the adrenal medulla and include serum cortisol, plasma ACTH, overnight dexamethasone suppression test, fractionated plasma catecholamines, 24-hour urine for metanephrine and normetanephrine, serum sodium, and potassium, plasma renin, serum aldosterone and adrenal androgens (serum DHEA-S).

CT and MRI provide important anatomic information in characterization of incidentalomas. CT densitometry, based on detecting the presence and amount of lipid within an adrenal mass, is useful for initial differentiation of adrenal adenomas from metastases. On unenhanced CT a density measurement <10 Hounsfield units (HU) defines a lipid-rich adenoma and has 71% sensitivity and 98% specificity for diagnosing a benign lesion.²⁹ If the mass is inhomogenous or has a density ≥ 10 HU, the diagnosis is uncertain (lipid-poor adenoma or malignant lesion) and contrast-enhanced CT scan is performed to assess the washout of initial enhancement in the lesion. Adenomas enhance significantly after the intravenous contrast administration and show more rapid washout of contrast than adrenal metastases. Standard contrast-enhanced CT images of the adrenal glands are obtained approximately 60 seconds after the beginning of bolus intravenous injection of contrast material, this being the only time when the attenuation value of adenomas and metastases are nearly identical. Adenomas have a much more rapid loss of enhancement, as early as 5 minutes after contrast injection, and attenuation values at 15 minutes after contrast administration can be used to differentiate adenomas from other masses: masses with an attenuation value less than 30 to 40 H on 15-minute delayed contrast-enhanced CT are almost always adenomas.³⁰ In addition to the delayed CT attenuation value itself, it is also possible to calculate the percentage washout of initial enhancement: the optimal threshold for enhancement washout at 15 minutes is 60%, resulting in a sensitivity of 88% and a specificity of 96% for the diagnosis of adenoma.³⁰

Chemical shift MRI also is used to differentiate adrenal adenomas from metastases, and it is the preferred anatomic imaging method in children and pregnant women. Any lipid-containing tissue shows a signal loss caused by cancellation of the signal from fat and water on opposed-phase compared with in-phase images. Visual analysis of in-phase and opposed-phase imaging for the detection of lipid within adrenal masses showed a sensitivity of 78% and specificity of 87% for diagnosing adrenal adenoma.³¹

Despite the excellent anatomic and structural detail the CT and MR techniques provide, functional adrenal imaging using targeted radionuclides, such as NP-59, MIBG, and FDG,

Table 8 Imaging in Hyperaldosteronism

Scintigraphic Pattern	Type of Aldosteronism
Symmetrical bilateral early imaging (before day 5)	Bilateral autonomous hyperplasia; secondary aldosteronism*
Unilateral early imaging (before day 5)	Unilateral adenoma (Conn's tumor) unilateral malignant aldosterone secreting tumor (rare)
Symmetrical late imaging (on or after day 5); nondiagnostic pattern	Normal adrenals; dexamethasone suppressible aldosteronism (rare)

*Should be excluded by measurement of renin and aldosterone levels and should not require imaging.

Table 9 NP-59 Scintigraphic Patterns in Incidentaloma

Scintigraphic Pattern	Etiology
Concordant	Benign (hypersecretory or non-secretory adenoma)
Discordant	Space-occupying lesions; adrenal cyst, myelolipoma, pheochromocytoma adrenal carcinoma, metastasis
Normal (symmetrical or nonlateralizing uptake)	Normal adrenal (mass not in adrenal) or adenoma <2 cm diameter

Concordant = uptake increased on side of the mass; discordant = uptake decreased on side of the mass.

offers the best diagnostic sensitivity and specificity for characterization of incidental adrenal lesions.

NP-59 scintigraphy has been effectively used to distinguish adrenal adenomas from nonadenomatous lesions (a diverse group including primary adrenal cancer, adrenal metastases, cysts, hematoma/hemorrhage, lipoma, myelolipoma and pseudoadrenal masses). Three distinct scintigraphic patterns are described (Table 9): concordant uptake (uptake greater on the side of the mass) is caused by a benign adrenal adenoma; the contralateral gland may show variable degree of suppression (Fig. 7); discordant uptake (absent, decreased or distorted uptake on the side of the mass) is caused by destructive and malignant processes (Fig. 8); normal uptake (symmetrical, nonlateralizing) occurs in pseudoadrenal masses (mass arises from another organ, such as pancreas, stomach, kidney); some lesions <2 cm may yield a nonlateralizing pattern because of the limited spatial resolution of scintigraphy; however, SPECT may be useful to identify small adrenal lesions.

The role of radionuclide imaging in evaluation of incidentally discovered nonsecretory adrenal masses has been unequivocally demonstrated.^{17,32,33} Because NP-59, MIBG and FDG target entirely separate physiologic processes, they can be used selectively, based on clinical setting and biochemical data, to identify different types of adrenal tumors.

Accurate in vivo tissue characterization by using different

radiotracers has been shown by Maurea and coworkers³² in 54 patients with incidentalomas. For characterizing an adrenal mass as an adenoma, NP-59 imaging had a positive predictive value of 89%; in contrast, the negative predictive value to rule out this type of tumor was 100%.

The positive predictive value of MIBG imaging for characterizing an adrenal mass as a chromaffin tumor was 83%, whereas the negative predictive value to rule out this type of tumor was 100%. FDG-PET was highly accurate for differentiating between benign and malignant adrenal lesions (sensitivity 100%, specificity 100%; Fig. 9). These results suggest that functional imaging can play a major role in noninvasive characterization of silent adrenal tumors. The authors propose that in patients without a history of cancer, functional imaging should start with NP-59 scintigraphy because benign cortical adenomas are the most common cause of non-secreting adrenal tumors. In the case of a normal NP-59 scan, MIBG should be used to assess for nonhypersecreting pheochromocytoma, and if negative should be followed by an FDG study. In patients with a history of malignancy, FDG-PET should be initially performed, and if negative should be followed by NP-59 and MIBG studies.³²

Another study comparing the results of MRI and radionuclide techniques (NP-59, MIBG, and FDG) for characterization of nonsecreting unilateral adrenal lesions evaluated 30 patients, among which 22 benign lesions (13 adenomas, 3

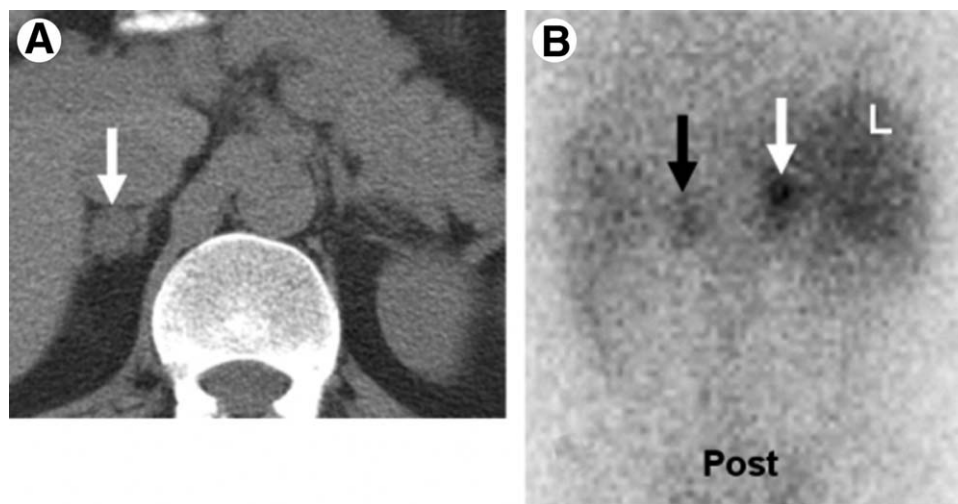


Figure 7 An incidentally discovered 1.8-cm diameter, right adrenal mass in a 37-year-old man. Abdominal CT (A) depicts the mass as lipid-poor with atypical contrast enhancement. NP-59 scintigraphy done without dexamethasone suppression (B) demonstrates a concordant pattern of imaging with right > left adrenal accumulation of iodocholesterol on the fifth and sixth days after injection compatible with a benign etiology. (Reprinted with permission from Gross et al.³)

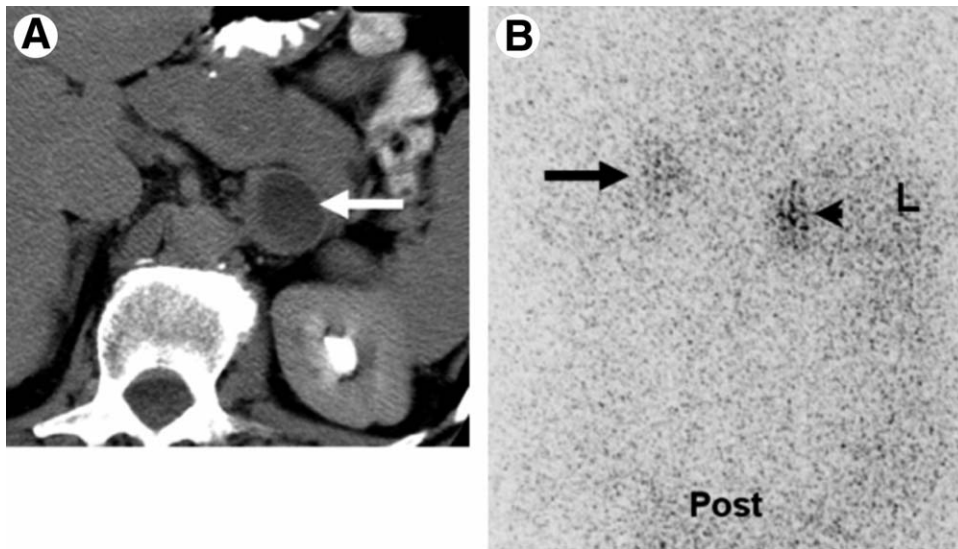


Figure 8 An incidentally discovered left adrenal mass with a discordant pattern of NP-59 imaging in a 61-year-old man 5 years after cystectomy and neobladder construction. Follow-up CT scans showed an enlarging left adrenal mass. Biochemical evaluation of adrenal function was normal. Subsequent laparoscopic adrenalectomy disclosed a pheochromocytoma. CT of the abdomen (A) showing a left adrenal mass (white arrow). NP-59 posterior (Pos) abdominal scan (B) showing faint normal liver tracer uptake (L) normal right adrenal tracer uptake (arrow head) and splayed left adrenal tracer accumulation compatible with a space-occupying adrenal mass (discordant pattern of imaging compatible with space occupying mass) (black arrow). (Reprinted with permission from Rubello et al.⁸ © 2002 Society of the European Journal of Endocrinology.)

cysts, 2 myelolipomas, and 4 pheochromocytomas) and 8 malignant lesions (4 adrenocortical carcinomas, 1 sarcoma, and 3 metastases) were finally diagnosed (based on histopathology, biopsy or 2-year clinical-imaging follow-up).³³ Qualitative MR evaluation showed T2 signal hyperintensity in 46% of adenomas and 100% of pheochromocytomas; signal intensity loss on chemical-shift imaging in 100% of adenomas; gadolinium enhancement in 100% of pheos and in

63% of malignancies. Radionuclide studies showed significantly increased NP-59 uptake only in adenomas, significant MIBG accumulation only in pheos, and focal FDG activity only in malignant adrenal lesions.³³

The excellent diagnostic performance of FDG-PET in differentiating malignant from benign adrenal lesions also was demonstrated by Yun and coworkers¹⁷ in a retrospective analysis of scans performed for 50 adrenal lesions in patients

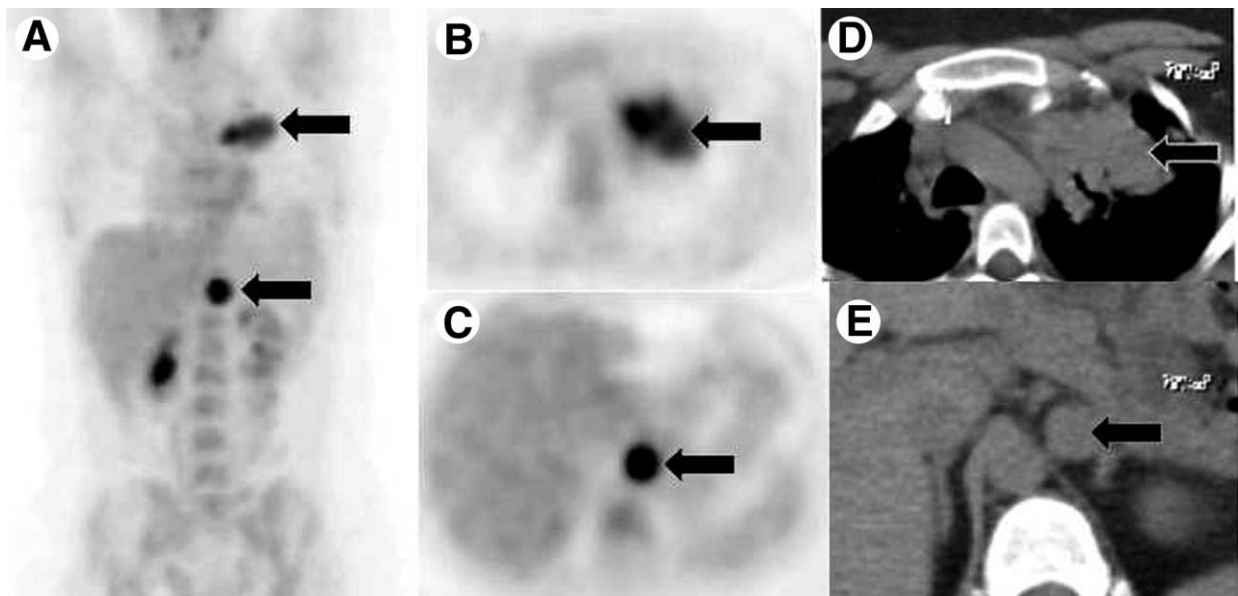


Figure 9 A left adrenal metastasis (arrow) depicted by FDG-PET/CT (A-C) in a patient with a non-small cell lung cancer (arrow). Corresponding chest (D) and abdominal (E) CT scans identifies the lung primary and the adrenal metastasis (arrow).

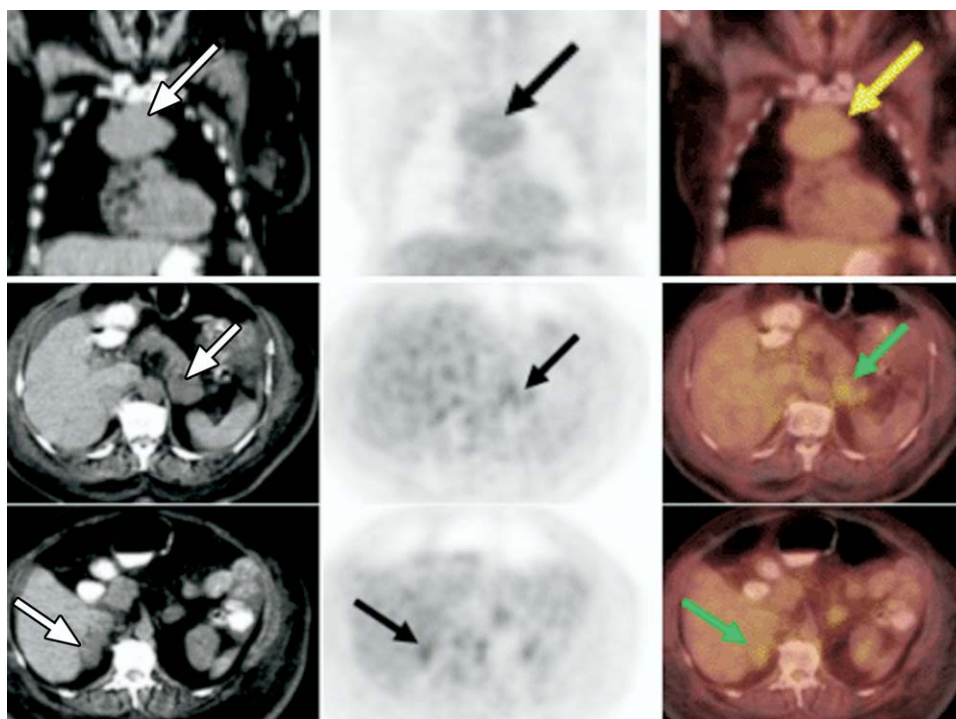


Figure 10 Bilateral adrenal enlargement seen on FDG-PET/CT scan of a 56-year-old woman with Cushing syndrome caused by ectopic ACTH secretion from a thymic carcinoid tumor; moderate FDG uptake is seen in the thymic carcinoid, likely related to the low metabolic rate of this tumor; the mild FDG activity in grossly enlarged adrenal glands is consistent with the benign nature of ACTH-induced hyperplastic adrenal enlargement. (Color version of figure is available online.)

with known or suspected malignancy: FDG-PET showed a sensitivity of 100%, a specificity of 94% and an accuracy of 96% for characterization of adrenal lesions. Unlike previously published studies that reported positive scan results when the lesion FDG uptake was greater than the background or blood-pool activity, yielding a sensitivity of 100% and specificity of 80% for detecting malignancy,³⁴ the authors interpreted the scans as positive when lesion FDG uptake was equal to or greater than the liver. This improved FDG-PET specificity, without compromising its sensitivity, for detecting malignant adrenal lesions.

Although high, the specificity of FDG-PET for detecting malignant adrenal lesions is not absolute, as demonstrated by several recent case reports illustrating focal FDG uptake in benign adrenal masses: a nonsecretory cortical adenoma,³⁵ an adenoma associated with subclinical Cushing's syndrome³⁶ and a giant adrenal myelolipoma.³⁷ These cases highlight the fact that integration of data from biochemical, anatomic and functional imaging, and sometimes histopathological examination is required for accurate characterization of adrenal masses (Fig. 10).

Functional Imaging of Adrenomedulla Tumors (Pheochromocytomas and Paragangliomas)

Pheochromocytomas are tumors arising from adrenal medulla, secreting excess catecholamine, and producing the clinical syndrome of hypertension associated with paroxys-

mal headache, palpitations, and sweating. These tumors also may be clinically silent and diagnosed during the biochemical and imaging workup of an adrenal incidentaloma. The detection of this type of tumor is critical, as up to 80% of patients with unsuspected pheochromocytoma who underwent surgery or anesthesia have died.²⁸ The presence of pheochromocytoma is established biochemically (fractionated plasma metanephrines, 24 hour urine for metanephrine and normetanephrine). Because approximately 90% of pheochromocytomas occur within the adrenal glands, CT has

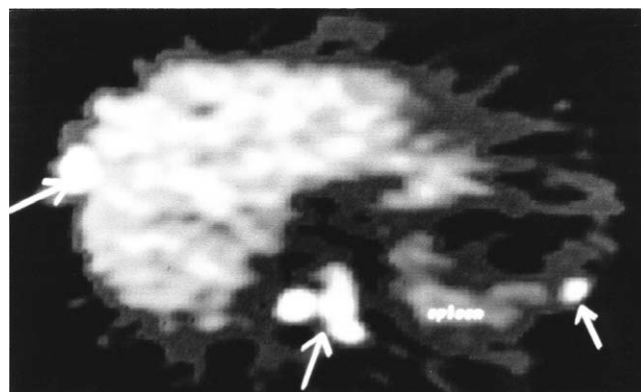


Figure 11 ¹¹C-Hydroxyephedrine (¹¹C-HED) PET scan in a patient with malignant pheochromocytoma. Multiple areas of increased uptake are seen in the liver, abdomen and spleen (arrows). (Reprinted with permission from Gross et al.³)

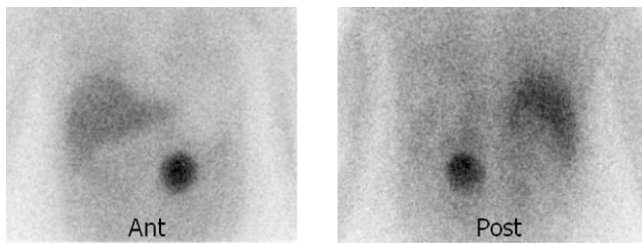


Figure 12 MIBG scan demonstrating intensely focal tracer activity in the left adrenal gland consistent with pheochromocytoma in a 56-year-old woman with hypertension, elevated plasma norepinephrine levels, and a 3-cm left adrenal mass seen on cross-sectional anatomic imaging.

been used as the primary imaging study. Most pheochromocytomas are readily detected on CT because they typically measure 2 to 5 cm. in diameter and display regions of necrosis or hemorrhage. Most pheochromocytomas have an unenhanced attenuation greater than 10 HU. Although administration of intravenous contrast was traditionally avoided in patients with known or suspected pheochromocytoma for fear of inducing a hypertensive crisis, newer nonionic IV contrast agents showed no significant increases in catecholamine levels in either control subjects or patients with pheochromocytomas.³⁸ Contrast-enhanced CT of adrenal pheochromocytoma commonly shows inhomogeneous enhancement of a solid mass, similar to the finding in adrenal metastasis or adrenal cortical carcinoma.

MRI is considered the anatomic imaging of choice for pheochromocytoma due to its excellent anatomic detail, the potential for better tissue characterization and the ability of imaging in multiple planes. On MRI, most pheochromocytomas are hypointense on T1-weighted images and markedly hyperintense on T2-weighted images. Although initial reports suggested that pheochromocytomas could be distinguished by their marked hyperintensity on T2-weighted im-

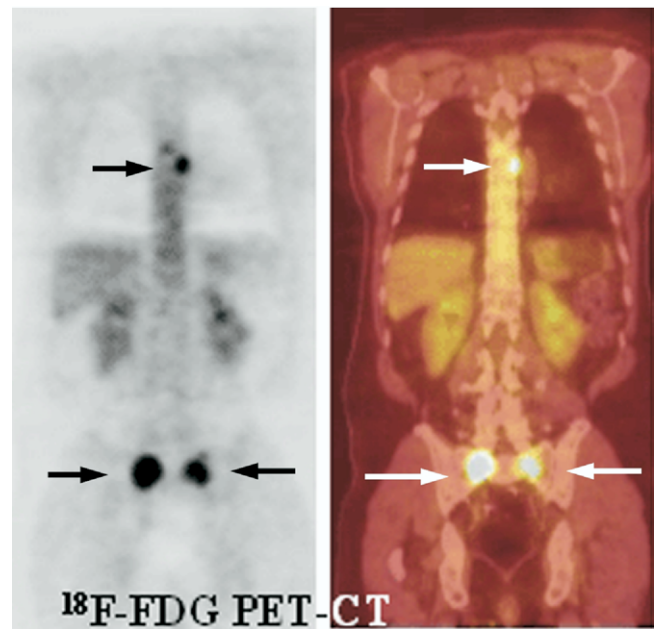


Figure 14 FDG-PET/CT scan demonstrating vertebral and bilateral sacral osseous metastases (arrows) in a 63-year-old man with negative MIBG scan and elevated plasma catecholamine levels who underwent resection of a pelvic paraganglioma 3 years previously.

ages, considerable overlap with other neoplasms, including adrenal cortical carcinomas, was demonstrated in up to 33% of cases.³⁹ Functional imaging of pheochromocytoma includes MIBG scintigraphy (using ¹³¹I or ¹²³I) and newer positron emitters ¹⁸F-FDA, ¹⁸F-DOPA, ¹¹C-epinephrine, and ¹¹C-hydroxyephedrine (Fig. 11).¹³

Sporadic intra-adrenal pheochromocytomas are depicted as intensely focal MIBG uptake (Fig. 12). MIBG scintigraphy is of particular value in imaging metastatic disease (the most common sites are the skeleton, lymph nodes, lung, and peri-

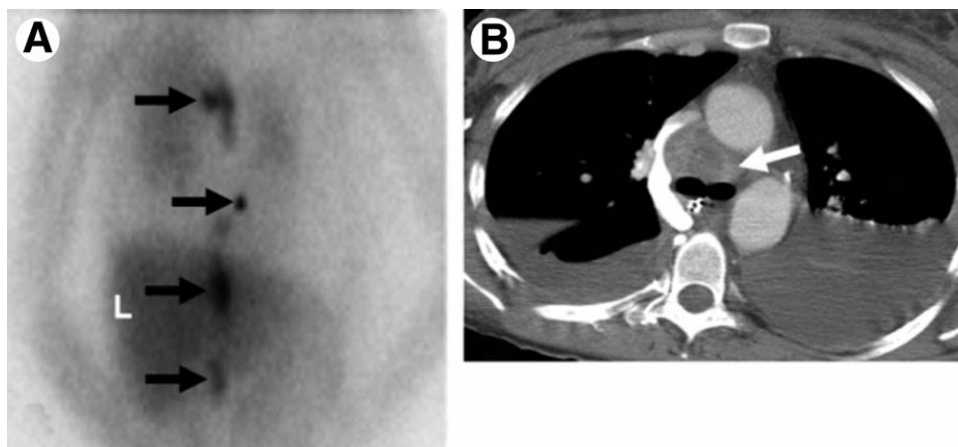


Figure 13 Malignant, metastatic pheochromocytoma demonstrated by ¹²³I-MIBG and CT in a 31-year-old woman after bilateral adrenalectomy and persistent hypertension complicated by renal insufficiency and recent development of superior vena cava obstruction. (A) Anterior chest and abdomen scan. L = normal liver uptake whereas arrows depict multiple, abnormal foci of ¹²³I-MIBG in metastatic pheochromocytoma deposits in the mediastinum and para-aortic regions. (B) Chest CT identifies the superior mediastinal mass responsible for SVC obstruction (white arrow). (Reprinted with permission from Rubello et al.⁸ © 2002 Society of the European Journal of Endocrinology.)

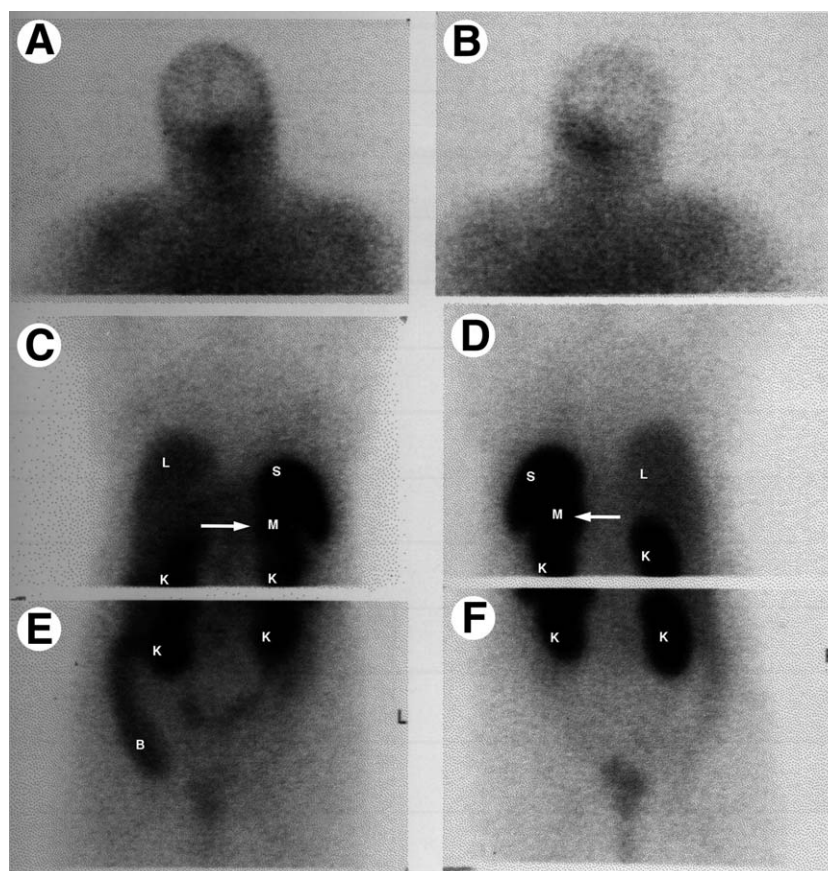


Figure 15 Anterior (A, C, E) and posterior (B, D, F) ^{111}In -pentetreotide scan depicting a sporadic left adrenal pheochromocytoma (arrow). K, kidney; L, liver; M, mass; S, spleen.

toneum) and in the localization of extra-adrenal pheochromocytomas (Fig. 13). These lesions occur at many locations from the base of the skull to the pelvis and are frequently not detected by computed tomography due to their small size and close relationship to other structures.⁴⁰ MIBG scintigraphy has demonstrated 87% sensitivity and 99% specificity for detection of pheochromocytomas.

Most pheochromocytomas, whether benign or malignant, are metabolically active, and can be imaged with FDG-PET. Shulkin and coworkers⁴¹ identified pheochromocytomas with FDG in 22 of 29 patients (76%), FDG uptake being more common in malignant than benign pheochromocytomas (Fig 14). Interestingly, some pheochromocytomas that poorly concentrated MIBG were well visualized with FDG, and all pheochromocytomas that failed to accumulate FDG were detected with MIBG.

Discordant results between FDG imaging and MIBG imaging, as well as ^{18}F -FDA imaging, were demonstrated in 5 patients with metastatic pheochromocytoma. Both ^{123}I MIBG and ^{18}F -FDA grossly underestimated the extent of disease when compared with CT and MRI. FDG-PET showed lesions not detected on either ^{123}I -MIBG or ^{18}F -FDA scans.¹⁵

When choosing the optimal imaging modality for pheochromocytoma, it is important to consider that approximately 25% of patients with apparently sporadic pheochromocytoma are carriers of germline mutations with a predisposition for extra-

adrenal and often multifocal disease; that in children 30% to 43% of pheochromocytomas are multifocal and extra-adrenal and that pheochromocytomas are malignant tumors in 26% to 35% cases.⁴² Because the benign or malignant behavior of pheochromocytoma cannot be conclusively predicted, it is recommended that initial localization of this tumor should be attempted by at least 2 different imaging modalities, one anatomic imaging technique to assess for structural details (such as tumor size, invasion in the renal vein or inferior vena cava, compression adjacent organs) and one functional imaging study to assess for primary or metastatic pheochromocytoma. The functional imaging test of choice is ^{123}I -MIBG (or ^{131}I -MIBG, if the former is not available). If the MIBG scan is negative, then PET using specific noradrenergic transporter system targeting such as ^{18}F -FDA and ^{18}F -DOPA should be employed. If these studies are negative, the tumor has likely undergone dedifferentiation with loss of specific type 1 uptake transporters and is probably malignant. In these instances imaging with FDG-PET or with ^{111}In -pentetreotide (Octreoscan) is recommended (Figs. 15 and 16).^{13,42}

Conclusion

Despite the importance of high-resolution anatomic imaging, the literature continues to document that functional adrenal scintigraphy is an important, integral part of the evaluation of patients with adrenocortical and adrenomedullary disease.

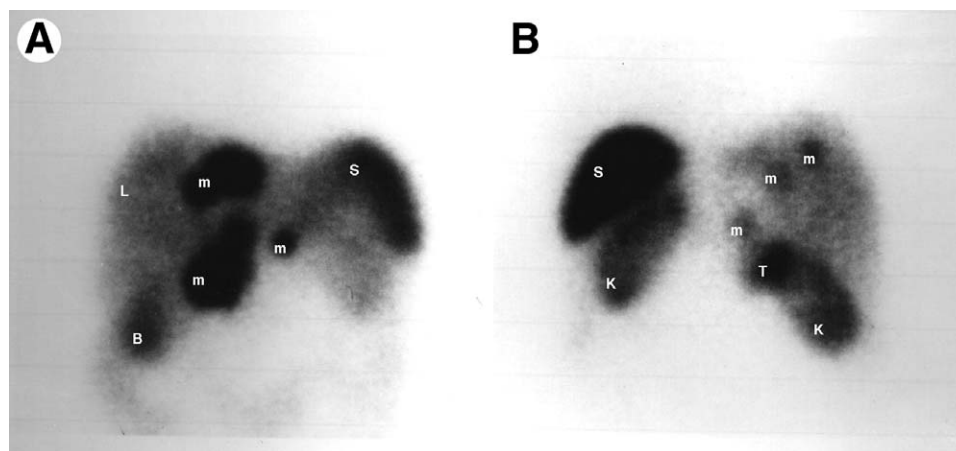


Figure 16 Anterior (A) and posterior (B) ^{111}In -pentetreotide scan in a patient with a malignant neuroendocrine tumor (T, tumor in right adrenal gland) and multiple liver metastases (m). B, bowel; L, liver; K, kidney; S, spleen.

Functional scintigraphy complements anatomy-based imaging and facilitates diagnostic localization. The creation of hybrid imaging devices, either PET or SPECT with CT will allow simultaneous functional and anatomic evaluation of adrenal dysfunction and will serve as the basis for the re-invention and exploitation of older radiopharmaceuticals and the impetus for the development of novel radiopharmaceuticals for adrenocortical and adrenomedulla imaging.

References

- Gross MD, Shapiro B, Bui C, et al: Adrenal scintigraphy and metaiodobenzylguanidine therapy of neuroendocrine tumors, in Sandler RE, Coleman JA, Patton FJ, et al (eds): *Diagnostic Nuclear Medicine* (ed 4). Philadelphia, Lippincott Williams and Wilkins, 2003, pp 715-734
- Gross MD, Bui C, Shapiro B: Adrenocortical scintigraphy, in Ell PJ, Gambhir SS (eds): *Nuclear Medicine in Clinical Diagnosis and Treatment* (ed 3). Edinburgh, Churchill and Livingstone, 2004, pp 45-52
- Gross MD, Korobkin M, Hussain H, et al: Adrenal gland imaging, in Jameson JL, DeGroot LJ (eds): *Endocrinology* (ed 5). Philadelphia, W.B. Saunders, 2005, pp 2425-2453
- Gross MD, Rubello D, Shapiro B: Is there a future for adrenal scintigraphy? *Nucl Med Commun* 23:197-202, 2002
- Gross MD, Valk TW, Thrall JH, et al: The role of pharmacologic manipulation in adrenal cortical scintigraphy. *Semin Nucl Med* 11:128-148, 1981
- Gross MD, Shapiro B: Scintigraphic studies in adrenal hypertension. *Semin Nucl Med* 19:122-143, 1990
- Shapiro B, Gross MD, Shulkin BL: Radioisotope diagnosis and therapy of malignant pheochromocytomas. *Trends Endocrinol Metab* 12:469-475, 2001
- Rubello D, Bui C, Casara D, et al: Functional scintigraphy of the adrenal gland. *Eur J Endocrinol* 147:13-28, 2002
- Gross MD, Shapiro B, Shreve P: Radionuclide imaging of the adrenal cortex. *Q J Nucl Med* 43:224-232, 1999
- Sisson JC, Frager MS, Valk TW, et al: Scintigraphic localization of pheochromocytoma. *N Engl J Med* 305:12, 1981
- Shapiro B, Wieland DM, Brown LE, et al: ^{131}I -meta-iodobenzylguanidine (MIBG) adrenal medullary scintigraphy: interventional studies, in Spencer RP (ed): *Interventional Nuclear Medicine*. New York, Grune & Stratton, 1983, pp 451-481
- Khafagi FA, Shapiro B, Fig LM, et al: Labetalol reduces iodine-131 MIBG uptake by pheochromocytoma and normal tissues. *J Nucl Med* 30:481-489, 1989
- Ilias I, Shulkin B, Pacak K: New functional imaging modalities for chromaffin tumors, neuroblastomas and ganglioneuromas. *Trends Endocrinol Metab* 16:66-72, 2005
- Ilias I, Yu J, Carrasquillo JA, et al: Superiority of 6-18F-fluorodopamine positron emission tomography versus ^{131}I metaiodobenzylguanidine scintigraphy in the localization of metastatic pheochromocytoma. *J Clin Endocrinol Metab* 88:4083-4087, 2003
- Mamede M, Carrasquillo JA, Chen CC, et al: Discordant localization of 2-[18F]-fluoro-2-deoxy-D-glucose in 6-[18F]-fluorodopamine- and [123I]-metaiodobenzylguanidine-negative metastatic pheochromocytoma sites. *Nucl Med Commun* 27:31-36, 2006
- Van der Harst E, de Herder WW, Bruining HA et al: 123I-Metaiodobenzylguanidine and ^{111}In -octreotide uptake in benign and malignant pheochromocytomas. *J Clin Endocrinol Metab* 86:685-693, 2001
- Yun M, Kim W, Alnafisi N, et al: 18F-FDG PET in characterizing adrenal lesions detected on CT or MRI. *J Nucl Med* 42:1795-1799, 2001
- Sohaib SA, Hanson JA, Reznick RH, et al: CT appearance of the adrenal glands in adrenocorticotropic hormone-dependent Cushing Syndrome. *AJR Am J Roentgenol* 172:997-1002, 1999
- Schteingart DE, Seabold JE, Gross MD, et al: Iodocholesterol adrenal tissue uptake and imaging in adrenal neoplasms. *J Clin Endocrinol Metab* 52:1156, 1981
- Fig LM, Ehrmann D, Gross MD, et al: The localization of abnormal adrenal function in the ACTH-independent Cushing syndrome. *Ann Intern Med* 109:547-553, 1988
- Gross MD, Freitas JE, Swanson DP, et al: Dexamethasone suppression adrenal scintigraphy in hyperandrogenism. *J Nucl Med* 22:12, 1981
- Nakajo M, Sakata H, Shinohara S: Positive imaging of arrhenoblastoma of the ovary with ^{131}I -aldosterol: case report. *Jpn J Nucl Med* 16:472, 1979
- Barkan AL, Cassorla F, Loriaux DL, et al: Steroid and gonadotrophin secretion in a patient with a 30-year history of virilization due to a lipoid-cell ovarian tumor. *Obstet Gynecol* 64:287, 1984
- Carpenter DC, Wahner HW, Salassa RM, et al: Demonstration of steroid producing gonadal tumors by external scanning with the use of NP-59. *Mayo Clin Proc* 54:332, 1979
- Pacak K, Eisenhofer G, Goldstein DS: Functional imaging of endocrine tumors: role of positron emission tomography. *Endocr Rev* 25:568-580, 2004
- Minn H, Salonen A, Friberg J, et al: Imaging of adrenal incidentalomas with PET using (^{11}C) -metomidate and (^{18}F) -FDG. *J Nucl Med* 45:972-979, 2004
- Zetting G, Mitterhauser M, Wadsak W, et al: Positron emission tomography imaging of adrenal masses: (^{18}F) -fluorodeoxyglucose and the 11beta-hydroxylase tracer (^{11}C) -metomidate. *Eur J Nucl Med Mol Imaging* 31:1224-1230, 2004

28. Kloos RT, Gross MD, Francis IR, et al: Incidentally discovered adrenal masses. *Endocr Rev* 16:460-484, 1995
29. Boland GW, Lee MJ, Gazelle GS, et al. Characterization of adrenal masses using unenhanced CT: an analysis of the CT literature. *AJR Am J Roentgenol* 171:201-204, 1998
30. Korobkin M, Brodeur FJ, Francis IR, et al. CT time-attenuation washout curves of adrenal adenomas and nonadenomas. *AJR Am J Roentgenol* 170:747-752, 1998
31. Outwater EK, Siegelman ES, Radecki PD, et al: Distinction between benign and malignant adrenal masses: value of T1-weighted chemical-shift MR imaging. *AJR Am J Roentgenol* 165:579-583, 1995
32. Maurea S, Klain M, Mainolfi C, et al: The diagnostic role of radionuclide imaging in evaluation of patients with nonhypersecreting adrenal masses. *J Nucl Med* 42:884-892, 2001
33. Maurea S, Caraco C, Klain M, et al: Imaging characterization of non-hypersecreting adrenal masses. Comparison between MR and radionuclide techniques. *Q J Nucl Med Mol Imaging* 48:188-197, 2004
34. Erasmus JJ, Patz EF Jr., McAdams HP et al: Evaluation of adrenal masses in patients with bronchogenic carcinoma using 18F-FDG PET. *AJR Am J Roentgenol* 168:1357-1360, 1997
35. Rao SK, Caride VJ, Ponn R, et al: F-18 fluorodeoxyglucose positron emission tomography-positive benign adrenal cortical adenoma: imaging features and pathologic correlation. *Clin Nucl Med* 29:300-302, 2004
36. Shimizu A, Oriuchi N, Tsushima Y, et al: High [18F] 2-fluoro-2-deoxy-D-glucose (FDG) uptake of adrenocortical adenoma showing subclinical Cushing's syndrome. *Ann Nucl Med* 17:403-406, 2003
37. Ludwig V, Rice MH, Martin WH, et al: 2-Deoxy-2-[18F]fluoro-D-glucose positron emission tomography uptake in a giant adrenal myelolipoma. *Mol Imaging Biol* 4:355-358, 2002
38. Mukherjee JJ, Peppercorn PD, Reznik RH, et al: Pheochromocytoma: Effect of nonionic contrast medium in CT on circulating catecholamine levels. *Radiology* 202:227-231, 1997
39. Francis IR, Korobkin M: Pheochromocytoma. *Radiol Clin N Am* 34: 1101-1112, 1996
40. Shapiro B, Sisson JC, Kalff V, et al: The location of middle mediastinal pheochromocytomas. *J Thorac Cardiovasc Surg* 87:814, 1984
41. Shulkin BL, Thompson NW, Shapiro B, et al: Pheochromocytomas: imaging with 2-[fluorine-18]fluoro-2-deoxy-D-glucose PET. *Radiology* 212:35-41, 1999
42. Ilias I, Pacak K: Current approaches and recommended algorithm for the diagnostic localization of pheochromocytoma. *J Clin Endocrinol Metab* 89:479-491, 2004